Two dimensional phase separation of diacetylenic matrix and glycolipids at the air–water interface

Zhanfang Ma,[a] Jinru Li,[ab] Hua Li[a] and Long Jiang*[a]

[a] *Laboratory of Colloid and Interface, Center for Molecular Science, Institute of Photographic Chemistry, Chinese Academy of Sciences, De Wai Bei Sha Tan, Da Tun Road 3A, Beijing 100101, P.R. China. Fax: + 86 10 64879735; E-mail: jianglng@public.bta.net.cn*

[b] *The State Key Laboratory of Transducer Technology, Institute of Electronics, Chinese Academy of Sciences, Beijing 100080, P.R. China*

Received (in Montpellier, France) 4th January 2000, Accepted 8th March 2000
Published on the Web 13th April 2000

The interaction between recognition elements (*e.g.*, receptors) and the photochromic diacetylenic matrix is of great importance in biosensor preparation. The characterization of the miscibility or phase separation of functionalized components is an indispensable step for the design and preparation of biosensors. The interactions between 2,4-tricosadiynoic acid (TCDA) and dioctadecyl glycerylether-β-glucosides (DGG) as well as 10,12-pentacosadiynoic acid (PCDA) and DGG were studied by surface pressure-area isotherms and Brewster angle microscopy. It has been found that for a mixed TCDA–DGG monolayer on water subphase, there existed good miscibility of TCDA and DGG. On the contrary, in a mixed PCDA–DGG monolayer, the miscibility of PCDA and DGG is poor; PCDA molecules easily separated from the mixed PCDA–DGG monolayer during compression and formed a branch-like pattern. This result is consistent with the result obtained in π–A isotherm and is discussed based on the different position of the diacetylene group in the molecules.

The study on self-assembled multicomponent membranes with functional units has become an important research field.[1–3] The characterization of the miscibility or phase separation of the monolayer components is a necessary step in the design and preparation of functionalized structures. The surface pressure (π) and average molecular area (A) isotherms can provide us with information on the interaction between molecules in monolayers.[4] In addition, Brewster angle microscopy (BAM) can provide us with effective and direct information about the 2D phase transition and the miscibility of the components in monolayers.

Polydiacetylenes can change their color from blue to red in response to various environmental perturbations, such as temperature,[5,6] pH,[7] mechanical stress[8–11] and solvent.[12] So polymer monolayers formed by lipids with the diacetylenic group have attracted particular attention due to their special photochromic properties.[13–15] Glycolipids are one of the major constituents in biological membranes and they play an important role in enhancing membrane stability and in transferring intercellular information.[16] Carbohydrates on the surface of cells serve as antenna for viruses, toxins, hormones and the other molecules in the recognition process on the surfaces of cells.[17] We have prepared polymer vesicles using 2,4-tricosadiynoic acid (TCDA) and 10,12-pentacosadiynoic acid (PCDA) as the matrix and dioctadecyl glycerylether-β-glucosides (DGG) as the receptor to detect *Escherichia coli* (*E. coli*).[18] Experimental results showed that the DGG–TCDA system was effective, however, the DGG–PCDA system was ineffective.

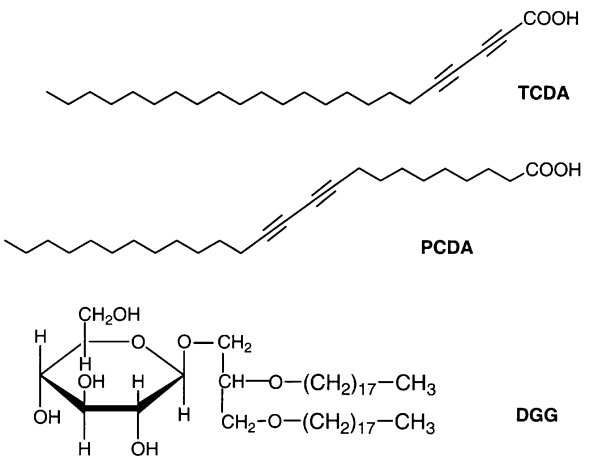

In the present study, to understand the phase transitions during the formation of the film composed of glycolipids and the diacetylenic matrix, the miscibility of mixed DGG–PCDA and DGG–TCDA binary monolayer films at the air–water interface was studied directly by means of Brewster angle microscopy.

Results

Surface pressure-area isotherms on a water subphase with different pH

From Fig. 1, we see that the smallest average molecular areas for both TCDA and PCDA monolayer films on the surface of water are at pH 5–7; these are characterized as solid-like films. However, collapse pressure and the limiting area per molecule of PCDA and TCDA are different. For PCDA the limiting area per molecule is about 27.9 Å^2 molecule^{-1}, with a collapse pressure at 15 mN m^{-1}; the limiting area of pure TCDA is about 20.9 Å^2 molecule^{-1}, with a collapse pressure at 55 mN m^{-1}. This demonstrates that the molecular area, which is related to the molecular structure, of PCDA is larger than that of TCDA. All of the following BAM experiments were done in a NaOH–NaH_2PO_4 buffer with pH 5.8.

BAM images of pure TCDA, PCDA, DGG and mixed DGG–TCDA, DGG–PCDA monolayers

Direct evidence about the miscibility or 2D phase separation of pure TCDA, PCDA and DGG and mixtures of TCDA–

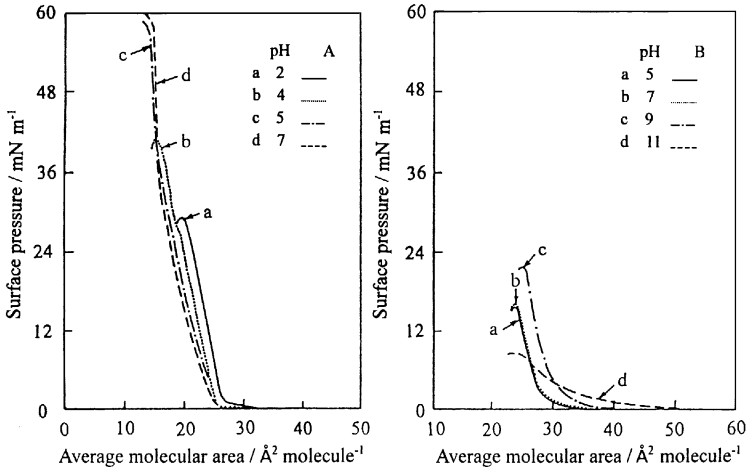

Fig. 1 The influence of pH on (A) TCDA and (B) PCDA monolayers at the air–water interface at 17.5 ± 0.5 °C.

DGG and PCDA–DGG in Langmuir monolayers is obtained by means of Brewster angle microscopy at the air–water interface. Imaging of the surface morphology was performed during continuously slow monolayer compression. Representative BAM images are selected at different surface pressures.

BAM images of pure DGG monolayers. Fig. 2 shows that aggregation of the DGG molecules at the air–water interface occurs during compression. There exists some irregular shape domains as shown in Fig. 2(*a*) ($\pi = 0$ mN m^{-1}), meaning that there is a strong tendency toward self-aggregation and domain formation. With the increase in surface pressure, the size and quantity of the domains also increase [shown in Fig. 2(*b*), 2(*c*)]. At high surface pressure, $\pi = 40$ mN m^{-1}, these domains coalesce and form a quite uniform monolayer, as shown in Fig. 2(*d*).

BAM images of pure TCDA and mixed DGG–TCDA monolayers. In pure TCDA at the beginning of compression, $\pi = 0$ mN m^{-1}, many round shaped domains were observed at the air–water interface, as shown in Fig. 3(*a*). On increase of surface pressure, the round shaped domains formed a net-shaped texture [shown in Fig. 3(*b*)]. At higher surface pressures, the substructure of the condensed phase TCDA domains gradually disappeared before their fusion into a homogeneous monolayer, as shown in Fig. 3(*c*) and 3(*d*).

However, the shape of the domains formed by the mixture of TCDA and DGG appeared chain-like [shown in Fig. 4(*a*)] quite different from that of domains formed by pure TCDA. On further compression, the net-shaped structure was observed [shown in Fig. 4(*b*) and 4(*c*)]. At high surface pressure, $\pi = 50$ mN m^{-1}, the uniform morphology of a monolayer was observed [shown in Fig. 4(*d*)]. From a comparison of Fig. 3(*d*) and 4(*d*) we can observe that the morphology of

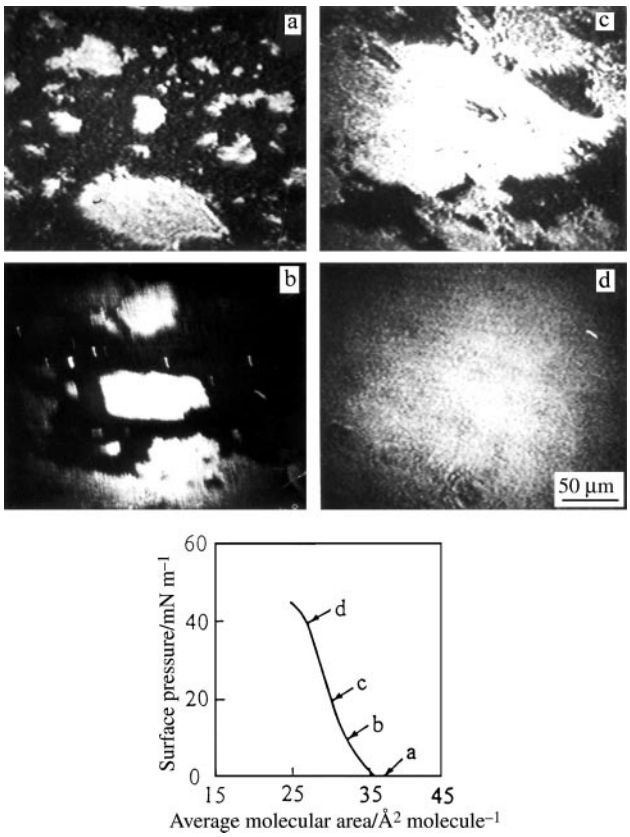

Fig. 2 BAM images of pure DGG monolayers at the air–water interface at (*a*) 0, (*b*) 10, (*c*) 20 and (*d*) 40 mN m^{-1} during compression.

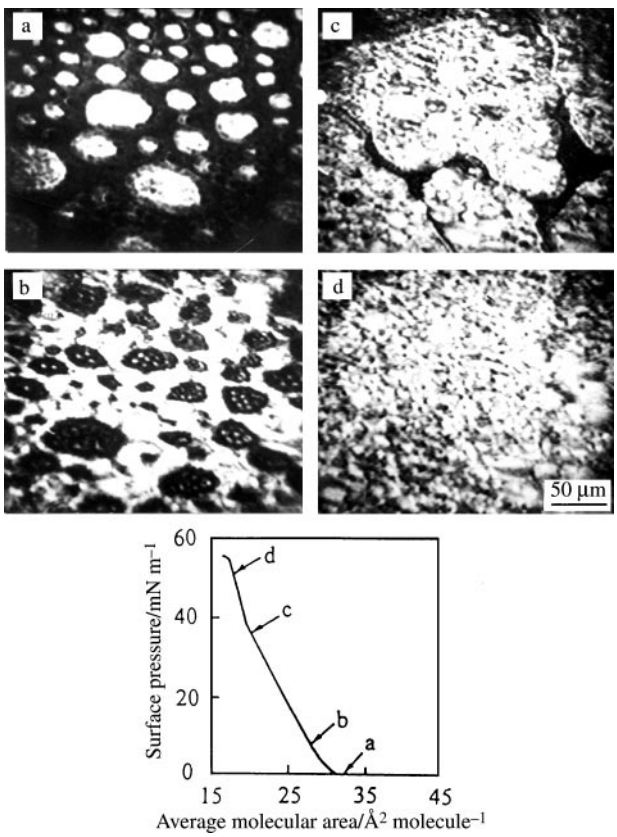

Fig. 3 BAM images of pure TCDA monolayers at the air–water interface at (*a*) 0, (*b*) 8, (*c*) 36 and (*d*) 52 mN m^{-1} during compression.

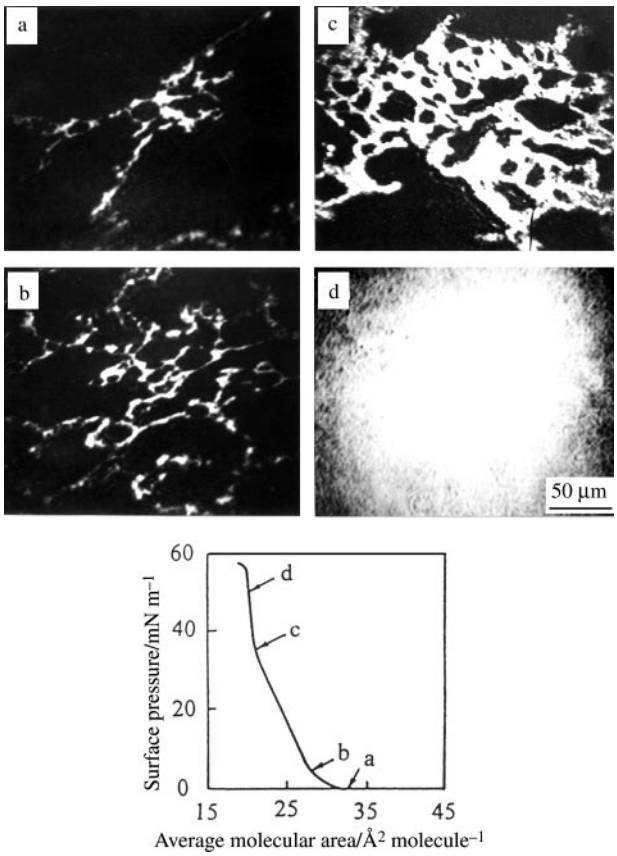

Fig. 4 BAM images of DGG–TCDA ($\chi_{DGG} = 0.2$) monolayers at the air–water interface at (*a*) 0, (*b*) 8, (*c*) 36 and (*d*) 52 mN m^{-1} during compression.

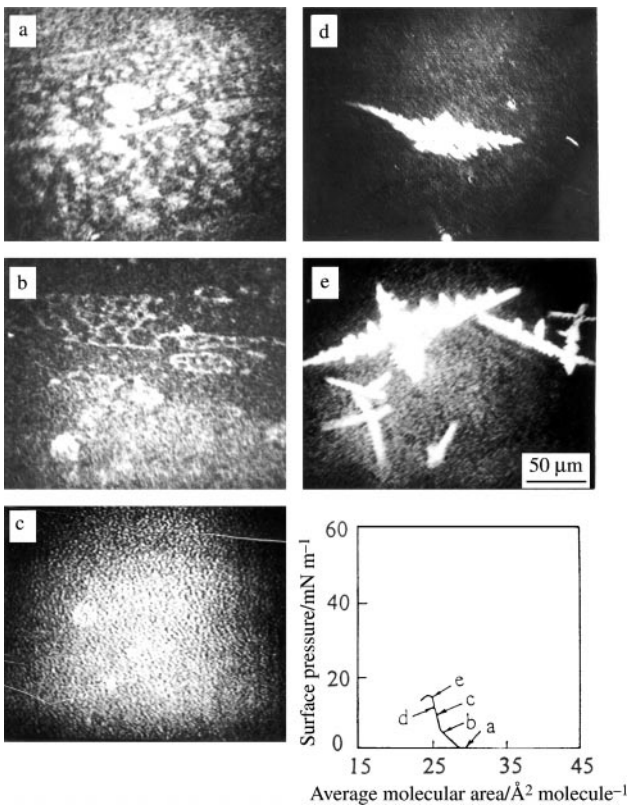

Fig. 5 BAM images of pure PCDA monolayers at the air–water interface at (*a*) 0, (*b*) 5, (*c*) 10, (*d*) 12 and (*e*) 14 mN m^{-1} during compression.

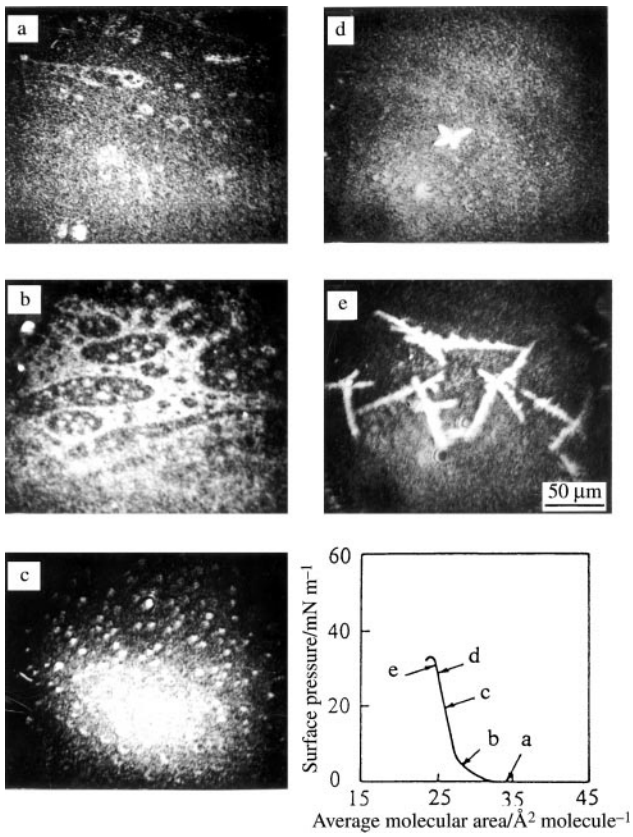

Fig. 6 BAM images of DGG–PCDA ($\chi_{DGG} = 0.2$) monolayers at the air–water interface at (*a*) 0, (*b*) 5, (*c*) 20, (*d*) 30 and (*e*) 32 mN m^{-1} during compression.

mixed TCDA–DGG monolayers is more uniform than that of pure TCDA monolayers on a water subphase. This demonstrates that there exists a strong interaction between DGG and TCDA, and the ability of TCDA to form a monolayer film is improved by the addition of DGG.

BAM images of pure PCDA and mixed DGG–PCDA monolayers. In pure PCDA, at $\pi = 0$ mN m^{-1}, many irregular shaped islands with different sizes can be observed [shown in Fig. 5(*a*)]. On increase of surface pressure these islands gradually formed irregular nets, as shown in Fig. 5(*b*). When $\pi = 10$ mN m^{-1} a homogeneous film was formed [shown in Fig. 5(*c*)]. On further compression obviously branch-shaped domains appeared [shown in Fig. 5(*d*)], whose number increased with pressure [Fig. 5(*e*)]. This might be the main reason that the PCDA monolayer has a very low collapse pressure ($\pi = 15$ mN m^{-1}).

For mixed PCDA–DGG monolayers, the phase transitions are similar to those of the pure PCDA system at low surface pressure (<10 mN m^{-1}) as shown in Fig. 6(*a*) and 6(*b*). At $\pi = 20$ mN m^{-1}, many protuberances could be observed on the surface of PCDA–DGG monolayers, as shown in Fig. 6(*c*). This proves that the miscibility of PCDA and DGG is poor. On further compression many branch-shaped domains, similar to those of the pure PCDA system, appeared [shown in Fig. 6(*d*), 6(*e*)].

Discussion

As we reported elsewhere,[19] for the TCDA–DGG system, the *negative* deviations of molecular areas from the additivity rule suggest strong attractive forces and good miscibility between TCDA and DGG. In contrast, for the PCDA–DGG system the *positive* deviations of molecular areas from the additivity rule indicate repulsive forces and poor miscibility between

PCDA and DGG. Our BAM observations further prove this conclusion.

The morphology of the TCDA monolayer was improved after the addition of DGG. However, the morphology of the PCDA–DGG monolayer was rougher than that of the pure PCDA monolayer [compare Fig. 5(*d*) and 6(*c*)]. This demonstrates that the miscibility of TCDA and DGG is better than that of PCDA and DGG. The addition of DGG increases the stability of both TCDA and PCDA monolayers, in particular for PCDA (the increase of the collapse pressure from 15 to 33 mN m^{-1}).

The attraction between amphiphiles arises mainly from hydrophobic forces and the repulsion arises mainly from the hydrophilic head-groups.[20] The main difference between PCDA and TCDA lies in the position of the diacetylenic group. In TCDA the rigid hydrophilic diacetylenic group is next to the carboxyl group. TCDA molecules are thus structurally composed of rigid hydrophilic head-groups and hydrophobic tails. Therefore, TCDA molecules can form very stable monolayer films. However, in PCDA the rigid hydrophilic diacetylenic group is in the middle of the lipid. This might weaken the interaction between hydrophobic tails, leading to a low-collapse pressure of the PCDA monolayer and poor stability of the PCDA-containing monolayer on a water subphase.

Conclusions

The experimental BAM results suggest that there is a good miscibility of TCDA and DGG. However, in a DGG–PCDA monolayer PCDA molecules separate from the mixed monolayer and a branch-like pattern is formed, showing that the miscibility of PCDA and DGG is poor. This different behavior results from the change in the position of the diacetylenic group in the lipids.

DGG molecules can enhance the stability of the monolayers of PCDA or TCDA on a water subphase, particularly for PCDA monolayers.

The BAM results are consistent with the results obtained from the pressure-area isotherms.

Experimental

PCDA and TCDA were purchased from Lancaster Co. (UK) and Dojindo Laboratories (Japan), respectively. They were not purified before use. Chloroform was purified before use and water used in the study was doubly distilled. DGG was synthesized in our laboratory according to the method described by Six *et al.*[21,22]

Pure and mixed DGG–PCDA, DGG–TCDA monolayers were dissolved in chloroform to a concentration of 1 mM. All surface pressure-area isotherms were measured with a Model HBM face membrane balance (Kaimen Kagaku Co. Ltd., Japan) at 17.5 ± 0.5 °C. The trough has an area of 800 cm^2 and the pressure sensor has a resolution of 0.1 mN m^{-1}. For each isotherm experiment, 200 μL of a 1 mM sample was spread on a water subphase and 10 min allowed for solvent evaporation before compression. The pH value of the subphase was adjusted with $NaOH–NaH_2PO_4$ buffer for pH > 5 and $HCl–C_6H_5(COOH)COOK$ buffer for pH < 5. The barrier was compressed at a speed of 20 cm^2 min^{-1}.

The morphology of the monolayers at the air–water interface was studied by means of a BAM set up by our group. The p-polarized beam of a He-Ne laser ($\lambda = 632.8$ nm) was directed at the Brewster angle (53.1°) at the air–water interface, giving a minimum surface reflectivity. The beams reflected from the monolayers were imaged by a CCD camera and recorded on videotapes for further analysis. One hundred microliters of a 1 mM sample was spread on the water subphase (pH 5.8, 17.5 ± 0.5 °C) and 10 min allowed for solvent evaporation before compression. BAM images were obtained during continuous slow monolayer compression and the morphological features were monitored with a lateral resolution of about 2 μm.

Acknowledgements

This study was financed by grants from the Chinese Academy of Sciences.

References

1 H. Kuhn, D. Mobius and H. Bucher, in *Physical Methods of Chemistry*, ed. A. Weissenberg and V. M. Rossiter, John Wiley, New York, 1972, vol. I, part IIIB.
2 A. Ulman, *An Introduction to Ultrathin Organic Films: From Langmuir–Blodgett to Self-assembly*, Academic Press, Boston, 1991.
3 G. G. Roberts, *Langmuir–Blodgett Films*, Plenum Press, New York, 1990.
4 G. X. Zhao, *Physical Chemistry of Surfactants*, Beijing University Press, Beijing, 1984, (in Chinese).
5 N. Mino, H. Tamura and K. Ogawa, *Langmuir*, 1992, **8**, 594.
6 H. Shibata, F. Kaneko, M. Aketagawa and S. Kokayashi, *Thin Solid Films*, 1989, **179**, 433.
7 R. R. Chance, G. N. Patel and J. D. Witt, *J. Chem. Phys.*, 1979, **71**, 206.
8 F. Kaneko, M. Shibata and S. Kobayashi, *Thin Solid Films*, 1992, **210**, 548.
9 R. A. Nallicheri and M. F. Rubner, *Macromolecules*, 1991, **24**, 517.
10 K. Tashiro, H. Nishimura and M. Kobayashi, *Macromolecules*, 1996, **29**, 8188.
11 V. K. Mitra and W. M. Risen, *J. Chem. Phys.*, 1977, **66**, 2731.
12 R. R. Chance, *Macromolecules*, 1980, **13**, 396.
13 D. H. Charych, J. O. Nagy, W. Spevak and M. D. Bednarski, *Science*, 1993, **261**, 585.
14 T. E. Wilson and M. D. Bednarski, *Langmuir*, 1992, **8**, 2361.
15 D. S. Johnston, L. R. McLean, M. A. Whittam, A. D. Clark and D. Chapman, *Biochemistry*, 1983, **22**, 3194.
16 A. Watts and J. J. H. M. De Pont, *Progress in Protein-Lipid Interactions*, Elsevier, Amsterdam, 1986, vol. 2.
17 S. Nathan and L. Halina, *Sci. Am.*, 1993, **1**, 75.
18 Z. F. Ma, J. R. Li, M. H. Liu, J. Cao, Z. Y. Zou, J. Tu and L. Jiang, *J. Am. Chem. Soc.*, 1998, **120**, 12678.
19 Z. F. Ma, J. R. Li and L. Jiang, *Langmuir*, 1999, **15**, 489.
20 J. N. Israelachivili, *Intermolecular and Surface Forces with Applications to Colloid and Biological Systems*, Academic Press, London, 1985, ch. 16.
21 L. Six, K. P. Rubeb and L. Lieflander, *J. Colloid Interface Sci.*, 1983, **93**, 109.
22 Y. K. Du, J. Y. An, J. A. Tang and L. Jiang, *Colloids Surf. B*, 1996, **7**, 129.